

RESEARCH ARTICLE**DESIGN, CONSTRUCTION, AND PERFORMANCE EVALUATION OF A SOLAR TUNNEL DRYER WITH AN AUXILIARY FLAT-PLATE SOLAR AIR HEATER FOR BITTER GOURD DRYING (*Momordica charantia*)**

P. Peratheepan¹, C. Nishan¹, F. C. Ragel¹

¹Department of Physics, Faculty of Science, Eastern University, Vantharumoolai, 30350, Sri Lanka

ABSTRACT

A solar tunnel dryer and an auxiliary solar air heating unit compatible with the tunnel dryer were designed and constructed. The solar tunnel dryer has a collector chamber and a drying chamber, which are separated by a board with holes in top for air circulation. The drying experiments were conducted for sliced bitter gourd (*Momordica charantia*) samples in the solar drying system with and without using the auxiliary air heating unit for eight hours in the premises of Eastern University. In order to compare and analyze the performance of the solar drying system, controlled drying experiments were also carried out in open sun on equal mass samples of bitter gourd kept adjacent to the solar drying system. The temperature profiles of the inlet, interface, and outlet of the solar tunnel dryer were compared with ambient temperature, and the wet basis moisture content obtained during the system drying were compared with the open sun drying. The performance of the dryer system has been investigated in terms of temperature profile in the drying area; moisture contents, moisture ratio and effective moisture diffusivity of bitter gourd samples with time of the day. Analysis on bitter gourd samples reveal that the system with the auxiliary air heating unit exhibits enhanced performance compared to the dryer without the auxiliary unit. The moisture ratio decreases exponentially as predicted by logarithmic model. The effective moisture diffusivity values of bitter gourd drying were determined based on Fick's Second Diffusion model.

Keywords: *Solar tunnel dryer, Open sun drying, Moisture content of bitter gourd, Moisture ratio, Effective moisture diffusivity*

DOI. <https://doi.org/10.4038/jsc.v14i1.61>



This is an open-access article distributed under the terms of the [Creative Commons Attribution 4.0 International License](https://creativecommons.org/licenses/by/4.0/), which permits unrestricted use, distribution and reproduction in any medium provided the original author and source are credited.

*Corresponding author: peratheepanp@esn.ac.lk

1. INTRODUCTION

Drying of agricultural products has been of great importance in food preservation for long time. Solar drying systems represent an alternative technique to traditional open sun drying and hot air drying. Open sun drying is not fast enough, thus leads to growth of microorganisms which will take place as a result of the relative high humidity, and harmful effects due to ultra-violet radiation [1]. On the other hand, the solar drying systems makes drying practically faster as a result the end product is clean, hygienic without the contamination of insects, microorganism and mycotoxin [2]. Therefore, the products can be worthily promoted to markets with high standards. With compared to open sun drying the solar drying deserves many advantages such as in saving drying time, increasing storage life-time, occupying less drying area, reducing field drying losses, and improving product quality in terms of colour, texture and taste.

Solar drying systems are now being widely used due to more energy efficient option. A variety of designs for solar drying systems have been developed and classified into direct, indirect, and specific solar dryers [3-5]. The solar dryers in tunnel, cabinet, and hybrid types are the commonly used dryers. In the direct type, the material to be dried is exposed directly to the sun radiation. In the indirect types of solar drying system, radiation does not directly incident on the material to be dried. Beside this, they operate more efficiently and have a great control over the drying process. Specific drying systems are generally designed with a specific feature and may be hybrid in nature. Drying systems may utilize heat transfer by convection, conduction, radiation, or a combination of these. The factors governing the rates of these processes determine the drying rate.

Even though, Sri Lanka is an agricultural country there isn't adequate technological advancement in turning the abundantly available green agricultural products such as brinjal, bitter gourd, tomato, cucumber, mushroom, carrot, potato, ginger, and red chili into value-added products. Bitter gourd (also known as *Momordica charantia* or bitter melon) is a bioactive natural product, which has rich source of carbohydrates, proteins, fibers, vitamins, and minerals. Traditionally it has been consumed as an indigenous medicinal food for preventing or controlling diabetic, healing wounds, preventing tumor, and boosting human immunity. *Understanding the intrinsic pharmaceutical properties of bitter*

gourd, we choose it as a drying product in this study to add value to the hugely cultivated bitter gourd in the eastern part of Sri Lanka.

In this study, we design and developed a low-cost solar tunnel dryer, which is suitable for a tropical country like Sri Lanka in which it can be exposed to long time solar radiation because of its configuration. In addition, with the intention of enhancing the drying efficiency of bitter gourd, a compatible and external auxiliary unit of a flat plate solar air heater was also designed and constructed. The performance of the constructed solar tunnel dryer was investigated as solar tunnel dryer being standalone model, as well as with the auxiliary unit of the solar air heater was attached to the solar tunnel dryer, and the results were compared upon bitter gourd drying in subsequent days.

2. MATERIAL AND METHODS

2.1 Design and Construction of Solar Tunnel Dryer

A portable solar tunnel dryer was designed and constructed using the available low-cost materials as described below. Fig. 1a shows the solar tunnel dryer, which consists of two chambers namely collector area and a drying area. This dryer was designed to maintain steady and nominal air flow by natural convection through the collector area and then to the dryer area, and thus in order to facilitate an upward flow of heated air of low density, the platform of the dryer was tilted by an angle of 7° from horizontal plane. The roof of the dryer was structured to be made out of corrugated Aluminum L-bars in gable shape in order to increase the area of solar irradiance, and it was tightly covered with UV stabilized semi-transparent polyethylene sheet of 200 micron thickness.

In order to minimize heat lost, the walls of the chambers were made using wooden slabs, and the collector and the drying chambers were partitioned with waterproof medium density fiberboard (MDF) board. A number of circular holes of diameter 4 cm were made evenly in the MDF board for air circulation. Zinc coated flat galvanized iron sheet of dimension $0.8 \times 0.5 \times 0.002$ m was cut and rare side was spray coated with clear black paint to provide improved heat absorption and hence enhanced thermal radiation. The Zinc coated iron sheet was then installed on top of a white polystyrene foam sheet of thickness 1.2 cm in the collector chamber. The polystyrene form sheets fixed in the chambers serve as a low-cost thermal insulator from loss due to convection and radiation. The sample drying tray of dimension $1 \times 0.45 \times 0.04$ m was prepared to hold the drying product in the

drying chamber, which has a wooden frame covered with black plastic mesh on top and steel mesh on bottom, which acts as shielding to block out thermal blackbody radiation. For the purpose of comparing the drying product in open sun drying, another tray was prepared with only black plastic mesh on top.



Figure 1: (a) The constructed solar tunnel dryer is in the field, and (b) when the auxiliary solar air heating unit is attached to the collector area of the solar tunnel dryer

2.2 Design and Construction of Flat-plate Solar Air Heater

The solar dryer system shown in Fig. 1b comprises an auxiliary unit of the flat-plate solar air heater, which was designed and constructed using locally available materials. The solar air heater has an opening in the front side and an enclosed channel track at the rear side. When using the auxiliary unit, the channel track can be adjoined to the opening of the collector chamber of the solar tunnel drier at an appropriate tilt angle, in order to send off the heated air passage into the collector of the dryer. The frame of the solar air heater was constructed using wooden sheets as low-cost durable thermal insulators. An absorber plate of V-grooved galvanized metallic sheet of dimensions of $0.8 \times 1.2 \times 0.1$ m was spray coated with clear black paint and then it was mounted on wedgings attached to the sides of the air heater. The absorber sheet was black painted in order to maximize the absorption of incident solar radiation. The gap between the absorber sheet and the base was compactly filled with dried wood dust as to provide good thermal insulation from the surrounding environment. The top of the solar air heater was covered with a transparent glass plate of 4 mm thickness, and the edges were tightly filled with silicone gel. The glass plate allows the incoming solar radiation to be transmitted and hence minimizes the heat losses due to convection and radiation. The metallic sheet of the absorber absorbs the solar radiation and acts as a black body radiator warming the air passes into the tunnel dryer through the air heater under natural convection.

2.3 Principle of the Solar Tunnel Drying

The solar tunnel dryer includes both direct and indirect drying. The air passage is provided on top and bottom of the collector area as well as drying area. Since the air passage is relatively small the volume of the air heated is correspondingly small, enabling the high rise in temperature as well as flow velocity and thus enhancing quick removal of moisture from the drying product. As the collector and the drying area are tilted the differential density arising from the heated air surges the lower density air passing upwards causing a natural airflow to the exit. On the other hand, the open sun drying basically occurs under hostile climatic conditions of solar radiation, ambient air temperature, relative humidity and wind speed.

2.4 Experimental Detail and Data Collection

The constructed solar tunnel dryer was installed at the courtyard of the Physics Department in the Eastern University, Sri Lanka, which is located at the *latitude and longitude coordinates of 7°48'0" N and 81°34'0" E*, respectively. In this study, fresh bitter gourds were purchased from the agriculture farm in the early morning of the day and were sliced into pieces of equal thickness of approximately 6 mm. The solar drying experiments were conducted in clear sunny days from 8.20 AM to 4.20 PM at ambient conditions till equilibrium moisture content is achieved in the solar tunnel drying. For comparison, the controlled experiments were also conducted with same weights of the sliced pieces of bitter gourd in open-sun drying. Figure 2 shows the bitter gourd samples prepared for drying experiments (Figure 2(a)), and the end products after drying in open sun drying (Figure. 2(b), side view) and in solar tunnel drying (Figure 2(c), top view).

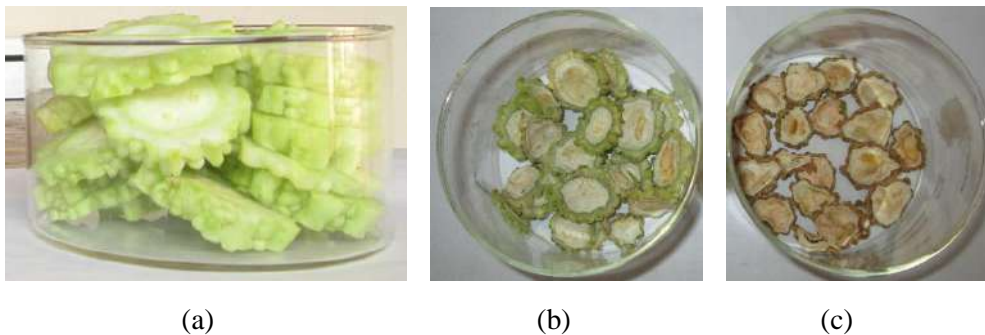


Figure 2: (a) Fresh bitter gourd chips prepared before drying, and the end products after drying for 8 hours in (b) open sun drying and in (c) solar tunnel drying

The initial weight of the sliced bitter gourd sample and weight at every 20 minutes of interval were measured to an accuracy of 0.01 g using an electronic balance. Air

temperature in the solar tunnel dryer at the inlet of the collector area, T_{inlet} ; at the interface of the collector/dryer areas, $T_{interface}$; and the out let of the dryer area, T_{outlet} were measured using thermometers with an accuracy of 0.5°C . The environmental temperature also was recorded simultaneously. The relative humidity and wind speed were measured at every drying interval of time using a wet and dry bulb hygrometer, and a wind cap anemometer, respectively.

3. RESULTS AND DISCUSSION

In the first experiment, the solar tunnel dryer was placed along the direction of the wind flow and the bitter gourd sliced sample were dried in it without using the auxiliary heating unit as shown in Figure 1(a). Then in second experiment that was done on the subsequent day, a fresh bitter gourd sliced sample were dried with the auxiliary heating unit as shown in Figure 1(b). Variations of temperature inside the solar tunnel dryer, the ambient temperature and relative humidity (RH) and the wind velocity against the ‘time of the day’ was measured in both experiments. Figure 3 shows the measured temperature profile, plotting the variation of the inlet temperature T_{inlet} , the outlet temperature T_{outlet} , and the interface temperature $T_{interface}$ between the collector and the dryer areas of the solar tunnel dryer without and with the auxiliary unit. For comparison, the ambient temperature $T_{ambient}$ also depicted in Figure 3. Figure 4 illustrates the variation of RH and wind speed against the ‘time of the day’ for both experiments.

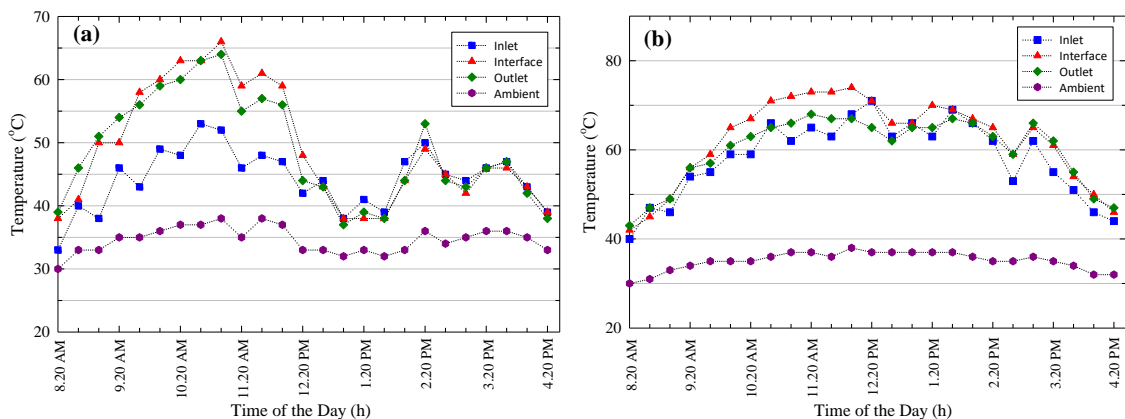


Figure 3: Variation of T_{inlet} , $T_{interface}$, T_{outlet} , and $T_{ambient}$ with local ‘time of the day’ during bitter gourd drying, (a) without using the auxiliary unit of the solar air heater and (b) using the auxiliary unit.

Figure 3 clearly distinguishes the temperature profile inside the solar tunnel dryer with reference to the ambient temperature without and with the auxiliary heating unit. It is

observed that the solar tunnel dryer at the interface attained a maximum temperature of 66°C at 11.00 AM, whereas the solar tunnel drying system with the auxiliary heating unit attained maximum of 74°C at 12.00 PM. It is also seen that the system with the auxiliary heating unit dries the bitter gourd sample by maintaining higher temperatures with better uniformity during the whole drying duration (average interface and outlet temperatures between 10.00 AM and 3.00 PM are 68.3°C and 64.7°C respectively) than the one without the auxiliary heating unit (average interface and outlet temperatures between 10.00 AM and 3.00 PM are 51°C and 49.9°C respectively). Moreover, the difference between the temperatures of the solar tunnel dryer and the ambient temperature is distinctly visible in the system with and without the auxiliary heating unit. The degree of heat driven from the auxiliary heating unit is evident from the temperature profile of the collector area of the solar tunnel dryer as seen in Figure 3(b). There is a visible drop in temperatures of the solar tunnel dryer roughly between 12.00 PM and 2.00 PM, which may be associated with the notable rise in the ambient RH observed in Figure 4(a) during this period of time. The difference between the solar tunnel dryer temperatures and the ambient temperature depends on various factors including buoyancy effect on the air flow [1, 6, 7], wind speed, RH, air flow rate, solar radiation, etc.

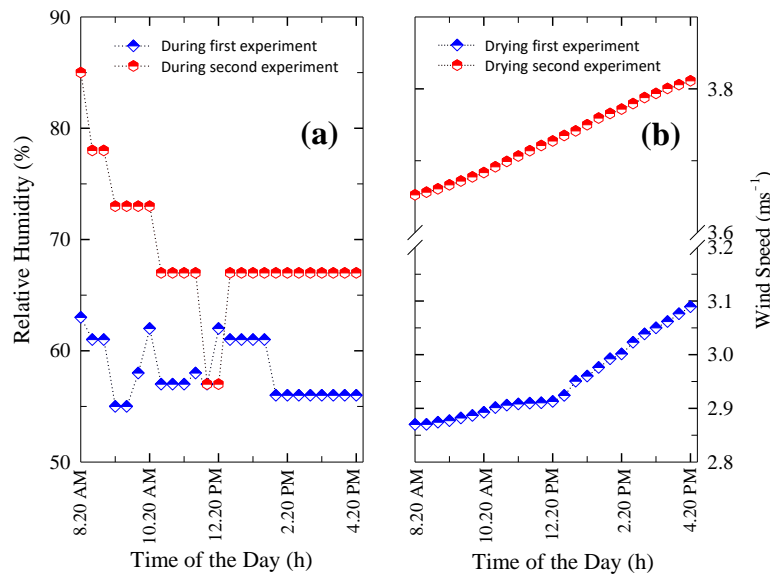


Figure 4. Variation of (a) ambient RH and (b) wind speed, against ‘time of the day’ for first and second experiments. The dotted lines are the guide to eye.

The wet basis moisture content MC_{wb} of the bitter gourd dried in the solar tunnel dryer and in open sun, were calculated according to

$$MC_{wb} = \frac{W_w}{W_w - W_{ds}} \times 100\%, \quad (01)$$

where W_w is the weight of the water content, and W_{ds} is the weight of the dry substance [8]. The variation of moisture content of bitter gourd against ‘time of the day’ is given in Figure 5 without the auxiliary heating unit (first experiment) and with the auxiliary heating unit (second experiment). The moisture content of the controlled experiments in open sun drying (as reference for the first and second bitter gourd drying experiments) of equal mass of the sliced bitter gourd samples are plotted in the same figure for comparison.

Although, the first and second experiments were conducted in clear and sunny successive days, the environmental conditions such as RH and wind speed are found to be in different as illustrated in Figure 4, which appears to influence the drying processes as observed in Figure 5. As evident in Figure 5, the removal of moisture content in bitter gourd sample of the first experiment without the auxiliary heating unit is observed to be higher than the second experiment with the auxiliary heating unit; in the first experiment, the equilibrium moisture content of the bitter gourd was determined to be 1.4% and 4.65% respectively under system drying (without auxiliary heating unit) and in open sun drying.

However, in the second experiment the respective values with auxiliary heating unit were determined to be 1.6% and 11.84%. This discrepancy can be understood by analyzing with respect to the controlled experiments (open sun drying) where the removal of water content from drying product is observed to be higher in the first experiment on the day where the relative humidity is lower than the second day experiment (average RH in the first and second days are 58.2% and 68.8%, respectively; see Figure 4). Studies show that RH has a major effect on dryer performance, where ambient and inlet humidity affects both drying kinetics and equilibrium moisture content, more pronouncedly at lower drying temperatures [9]. Studies also show that increased RH intensifies heat transfer process while decreased RH intensifies mass transfer process; moreover, controlled high RH in the initial drying stage and then decreasing RH can improve drying efficiency [10]. This study further shows that low RH increases drying rate so that material surface generates a rigid crust or shell that fixes the volume.

Therefore, it is evident that the difference in RH and wind speed in two different days that is seen in Figure 4 do influence the first and second experiments as noticeable in Figure 5, and hence in order to reliably compare the effectiveness of the solar tunnel dryer without and with the auxiliary heating unit, it is required to calculate the removal of MC in the bitter gourd sample in the dryer relative to open sun drying as

$$\Delta(MC) = MC \text{ of the sample in open drying} - MC \text{ of the sample under solar tunnel system drying} \quad (02)$$

which is portrait in the insert in Figure 5. As seen in the insert, the system with the auxiliary heating unit shows higher removal of MC than in the system without the auxiliary heating unit after reaching sufficiently higher temperature in the drying area of the solar tunnel dryer after about 3 hours of drying time.

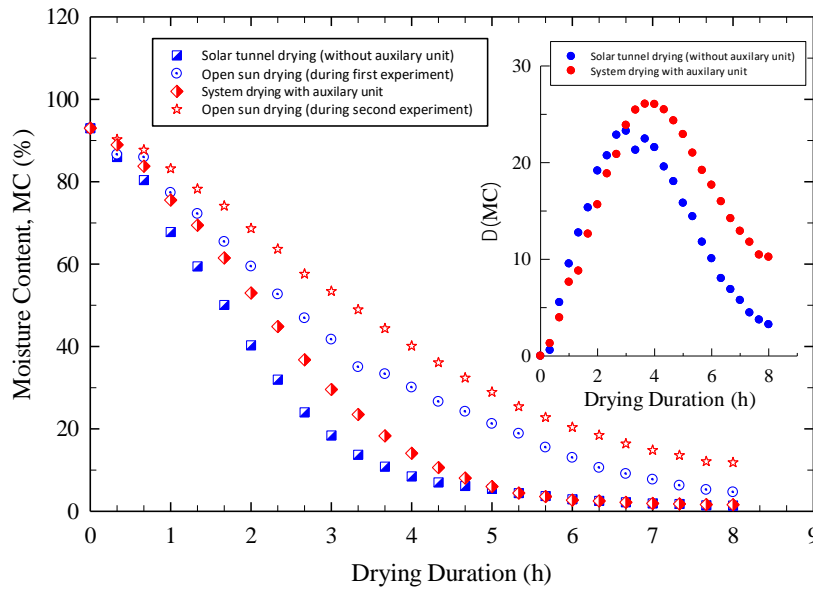


Figure 5: Variation of moisture content of bitter gourd in the (a) first experiment in solar tunnel dryer without the auxiliary heating unit (square symbol); (b) second experiment in solar tunnel dryer with auxiliary heating unit (diamond symbol); and (c) controlled experiments for first and second experiments in open sun (open symbols). The insert gives a measure of MC removal from bitter gourd samples in the solar dryer without and with auxiliary heating unit relative to open sun drying as calculated using Eq. (02).

The dimensionless moisture ratio (MR) of a drying substance is expressed by

$$MR = \frac{(MC)_t - (MC)_e}{(MC)_0 - (MC)_e}, \quad (03)$$

where $(MC)_e$ is the moisture content at any time, and $(MC)_e$ is the equilibrium moisture content, and $(MC)_0$ is the initial moisture content. In order to eliminate the effects of continuous fluctuations of the relative humidity of drying air in the drying process, the Eq. 03 can be simplified to the form of $MR = (MC)_t/(MC)_0$. [11]. The MR of bitter gourd samples were determined from the data of the wet basis moisture content presented in Figure 6. The MR of bitter gourd dried in solar tunnel dryer without and with the auxiliary heating unit are plotted in Figure 6 as a function of drying time, together with the data obtained simultaneously in open sun drying during both experiments. The MR of bitter gourd sample decreases exponentially nearly after 1.5 and 2 hours of drying in solar tunnel dryer without and with the auxiliary heating unit. The predicted moisture ratio was determined using the following expression of the logarithmic model [12]

$$MR_{\text{Predicted}} = \frac{(MC)_t}{(MC)_0} = a \exp(-kt) + c, \quad (04)$$

where a , k , and c are the coefficients. The dashed lines in Figure 6 are the simulated fits to the experimental data from the non-linear regression analyses using Eq. 04. The extracted fit coefficients and the resulting Sigma Plot parameters are summarized in Table 1. The coefficient of determination (R^2 -value) of the fits indicates the suitability of the mathematical model (Eq. 04) used for describing the drying behavior of bitter gourd samples in the solar tunnel dryer system. The lower the value of Standard Error of Estimate (SEE) credits the better the goodness of the fits obtained. Hence, it offers conformity between the experimental and predicted moisture ratios, in both experiments. It should be noted that the fit deviates from the experimental data in the beginning of drying, which may be because certain amount of heat is absorbed by the samples to exceed its latent heat of evaporation to promote smooth drying.

Table 1: Results of the analyses on the Logarithmic modelling of Eq. (04) for solar tunnel drying of bitter gourd, without and with the auxiliary air heating unit

Condition of experiment	Conduction	A	K	C	R ²	SEE
Without auxiliary heating unit		2.1893	0.6492	-0.0079	0.9962	0.0113
With auxiliary heating unit		1.9857	0.7862	0.0128	0.9985	0.0063

The effective moisture diffusivity (D_{eff}) of the bitter gourd samples was determined using the Fick's simplified mathematical model [11]. The solution of Fick's second law for a slab geometry is as follows [13]

$$MR = \frac{(MC)_t - (MC)_e}{(MC)_0 - (MC)_e} = \frac{8}{\pi^2} \sum_{n=1}^{\infty} \frac{1}{(2n+1)^2} \exp\left(\frac{-(2n+1)^2 \pi^2 D_{\text{eff}} t}{4H^2}\right), \quad (05)$$

where H is the half-thickness of the slab in sample in m , and n is a positive integer, and D_{eff} is expressed in m^2s^{-1} . The solution was found with the assumption of moisture migration being by diffusion, negligible shrinkage, constant diffusion coefficients and temperature [14]. For prolong drying, the Eq. (05) can be further simplified (by setting $n = 1$) to a straight line expression as

$$\ln(MR) = \ln\left[\frac{(MC)_t}{(MC)_0}\right] = \ln\left(\frac{8}{\pi^2}\right) - \left(\frac{\pi^2 D_{\text{eff}} t}{4H^2}\right). \quad (06)$$

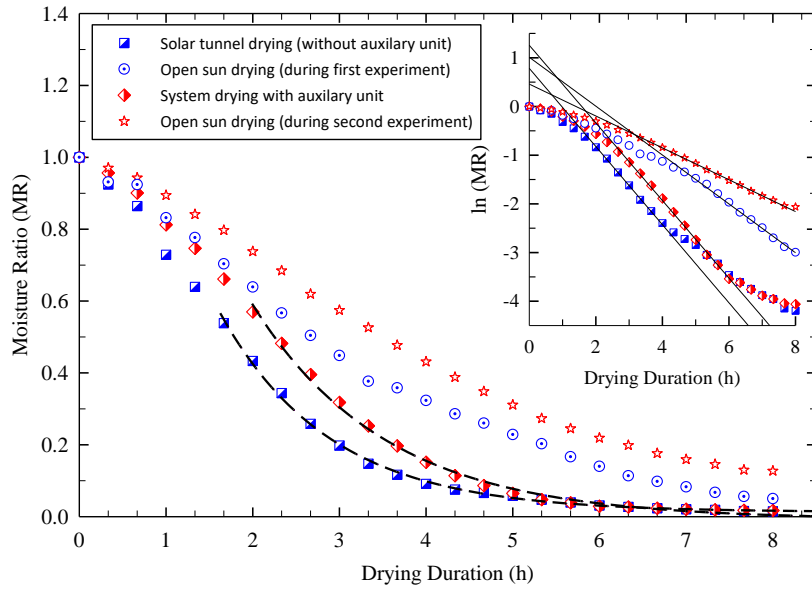


Figure 6: Variation of moisture ratio of bitter gourd samples determined in the (a) first experiment in solar tunnel dryer without the auxiliary heating unit (square symbol); (b) second experiment in solar tunnel dryer with auxiliary heating unit (diamond symbol); and (c) controlled experiments for first and second experiments in open sun (open symbols). The dotted lines are the simulated fits to Eq. (04). The inset is the plot of $\ln(MR)$ versus drying duration, where the symbols follow the identical labeling of MR, and the solid lines are the fits to Eq. (05).

The experimental data is plotted in the scheme of $\ln(D_{\text{eff}})$ versus drying duration, t in the inset in Figure 6. As seen from the inset in Figure 6, the solar tunnel drying in both experiments show linear region at intermediate duration of drying, whereas the open sun

drying experiments show at latter duration of drying. Thus, the linear regions of the curves were fitted to Eq. 05, and hence the D_{eff} values were calculated from the gradient ($\pi^2 D_{\text{eff}} / 4H^2$) of the plots and using H value of 3×10^{-3} m. The extracted values of the gradient (m) and the intercept (c_i), as well as the calculated D_{eff} values are summarized in Table 2. Among the different drying approaches, the system without the auxiliary heating unit offered slightly high value of D_{eff} than that the one with the auxiliary heating unit. This finding substantiates with the observed MC and MR that are presented in Figure 5 and Figure 6 respectively. Moreover, the drying of bitter gourd samples in the solar tunnel dryer system yield predominantly higher D_{eff} values compared to open sun drying, demonstrating the effectiveness of the system for bitter gourd drying. The D_{eff} values obtained for bitter gourd drying in our solar tunnel dryer are higher than the values reported for bitter gourd drying by various methods in the literature: $4.05 \times 10^{-8} \text{ m}^2\text{s}^{-1}$ in solar cabinet drying [15]; $1.91 \times 10^{-9} \text{ m}^2\text{s}^{-1}$ in air oven drying followed by treating it in NaCl solution [16], and $9.15 \times 10^{-10} \text{ m}^2\text{s}^{-1}$ by hot air drying [17].

Table 2: Fit parameters of Eq. 05 and the calculated values of effective diffusivity (D_{eff})

Experimental Condition	M	c_i	D_{eff} ($10^{-6} \text{ m}^2\text{s}^{-1}$)
System drying without auxiliary heating unit	0.8026	0.7842	2.92
Open sun drying during first experiment	0.5019	1.0118	1.83
System drying with auxiliary heating unit	0.7969	1.2577	2.90
Open sun drying during second experiment	0.3274	0.4604	1.19

CONCLUSION

In this study, a solar tunnel dryer and a compatible auxiliary air heating unit were constructed, and experiments were conducted for bitter gourd drying in the constructed solar tunnel dryer system with and without the auxiliary heating unit, and open sun drying was also done for equal mass bitter gourd samples as reference. The performance of the dryer system was investigated in terms of moisture contents, moisture ratio and effective moisture diffusivity of bitter gourd samples with time of the day. The measured temperature profiles of the two experiments reveal that the solar tunnel dryer with auxiliary heating unit maintains a higher average temperature of 68.3°C and 64.7°C in the interface and outlet respectively in the dryer area between 10.00 AM to 3.00 PM, while the dryer without the auxiliary heating unit maintains an average temperature of 51°C and 49.9°C

respectively for the same. Analysis of moisture content of bitter gourd samples dried in the dryer with respect to open sun drying reveals that the ambient relative humidity and the wind speed are found to influence the drying kinetics. Moreover, analysis on bitter gourd samples reveal that the system with the auxiliary heating unit exhibits enhanced removal of moisture content than in the system without the auxiliary heating unit. It is also shown that the moisture ratio decreases exponentially with drying time, well corroborating with mathematical model reported in the literature. The effective moisture diffusivity values of bitter gourd drying determined based on Fick's Second Diffusion model are compared with values reported in the literature.

REFERENCE

- [1] Stiling J, Li S, Stroeve P, Thompson J, Mjawa B, Kornbluth K, Barrett D.M. (2012), Performance evaluation of an enhanced fruit solar dryer using concentrating panels, *Energy for Sustainable Development* **16**: 224-230.
- [2] Bala B.K, Mondol M.R.A, Biswas B.K, Das Chowdury B.L, Janjai. S. (2003) Solar drying of pineapple using solar tunnel drier, *Renewable Energy* **28**: 183-190.
- [3] Mujumdar AS. (1995) *Handbook of Industrial Drying*. New York: Marcel Decker Inc.
- [4] Irtwange S.V and Adebayo S (2009) Development and performance of a laboratory-scale passive solar grain dryer in a tropical environment, *Journal of Agricultural Extension and Rural Development* **1**: 042.
- [5] Chow T.T (2010) A review on photovoltaic/thermal hybrid solar technology, *Applied Energy* **87**: 365.
- [6] Bolaji Bukola B, Olayanju, T.M.A.; Falade T.O. (2011) Performance evolution of a solar wind-ventilated cabinet dryer, *The West Indian Journal of Engineering* **33**: 12-18.
- [7] El-Sebaii A.A, Shalaby S.M. (2011) Solar drying of agricultural products: A review, *Renewable and Sustainable Energy Reviews* **16**: 37-43.
- [8] AOAC, *Official Methods of Analysis*, Association of Official Analytical Chemists International. (2005) Washington DC, WA, USA.
- [9] Kemp I. C (2007) Humidity Effects in Solids Drying Processes, *Measurement and Control* **8**: 268-281.

- [10] Zhang W.P, Yang X.H, Mujumdar A.S, Ju H.Y, and Xiao H.W. (2022) The influence mechanism and control strategy of relative humidity on hot air drying of fruits and vegetables: A review, *Drying Technology* **40**: 2217–2234.
- [11] Diamante L.M, and Munro P.A. (1993) Mathematical modelling of the thin layer solar drying of sweet potato slices, *Solar Energy* **51**: 271-276.
- [12] Togural I.T, and Pehlivan D. (2003) Modeling of drying kinetics of single apricot, *Journal of Food Engineering* **58**: 23-32.
- [13] Okos M.R, Narsimhan G, Singh R.K, and Weitnauer A.C. (1992) Food dehydration, In. D.R. Heldman, and D. B. Lund (Eds.) *Handbook of Food Engineering*, 462.
- [14] Crank J. (1975) *Mathematics of diffusions* (2nd ed.). London: Oxford University Press.
- [15] Jadhav B, Visavale G.L, Sutar P.P, Annapure U.S, and Thorat B.N. (2010) Solar Cabinet Drying of Bitter Gourd: Optimization of Pretreatments and Quality Evaluation, *International Journal of Food Engineering* **6**: 1-18
- [16] Biswas I. Mandal S. Samadder M, Mukherjee S. (2018) Drying characteristics of bitter gourd (*Momordica charantia*), *Journal of Crop and Weed* **14**: 111-116.
- [17] Yang L, Hu Z, Yang L, Xie S, Yang M. (2018) Hot-air drying characteristics and quality evaluation of bitter melon slice, *INMATEC-Agricultural Engineering* **55**: 53-62.